Hydrothermal Germination Models: Comparison of Two Data-Fitting Approaches with Probit Optimization

Article *in* Crop Science · September 2015

DOI: 10.2135/cropsci2014.10.0703

6 authors, including:

Christina Walters
United States Department of Agriculture
149 PUBLICATIONS **5,527** CITATIONS
SEE PROFILE

Alex Boehm
United States Department of Agriculture
7 PUBLICATIONS **36** CITATIONS
SEE PROFILE

Peter J. Olsoy
Washington State University
15 PUBLICATIONS **113** CITATIONS
SEE PROFILE

Patrick E. Clark
United States Department of Agriculture
73 PUBLICATIONS **1,052** CITATIONS
SEE PROFILE

Published August 17, 2015

RESEARCH

Hydrothermal Germination Models: Comparison of Two Data-Fitting Approaches with Probit Optimization

Stuart P. Hardegree,* Christina T. Walters, Alex R. Boehm, Peter J. Olsoy, Patrick E. Clark, and Frederick B. Pierson

ABSTRACT

Probit models for estimating hydrothermal germination rate yield model parameters that have been associated with specific physiological processes. The desirability of linking germination response to seed physiology must be weighed against expectations of model fit and the relative accuracy of predicted germination response. Computationally efficient empirical models have been proposed that do not require a priori assumptions about model shape parameters, but the accuracy of these models has not been compared to the more common probit-optimization procedure. Thirteen seedlots, representing six native perennial rangeland grasses and an invasive annual weed, were germinated over the constant temperature range of 3 to 36°C and water potential range of 0 to −2.5 MPa. Hydrothermal germination models were generated using probit optimization, optimized regression, and statistical gridding. These models were evaluated for the pattern and magnitude of residual model error and the relative magnitude of predictive errors under field-simulated temperature and moisture conditions. Residual model errors in predictions of germination rate were greatest for the probit optimization procedure. Statistical gridding and optimized regression produced lower predictive model error, but the latter procedure could not resolve germination response for slower-germinating seed populations. The more computationally efficient and accurate regression and statistical-gridding procedures may be desirable for identifying germination strategies and syndromes that are based on predicted response to simulated conditions of field temperature and moisture.

S. Hardegree, A. Boehm, P. Clark, and F. Pierson, USDA–ARS, Northwest Watershed Research Center, Boise, ID 83712; C. Walters, USDA–ARS, National Center for Genetic Resources Preservation, Fort Collins, CO 80521; and P. Olsoy, Boise Center Aerospace Lab., Boise State Univ., Boise, ID 83725. This work was supported by the Bureau of Land Management Intermountain Greenstripping and Rehabilitation Research Project (agreement no. USDI/BLM 60-91H2-8-0020), USDA National Institute of Food and Agriculture (grant nos. AFRI-60-5360-2-832, AFRI-58-5362-3-001), and the USDA–ARS Ecologically Based Invasive Plant Management program. Mention of a trade name or proprietary product does not constitute endorsement by USDA or a recommendation over other products that may be suitable. USDA is an equal opportunity provider and employer. Received 14 Oct. 2014. Accepted 9 Feb. 2015. *Corresponding author (stuart.hardegree@ars.usda.gov).

Abbreviations: ψ, water potential; PO, probit optimization; REG, optimized regression; RMSE, root mean square error; SG, statistical gridding; *T*, temperature.

Wildland plants in the semiarid western United States experience high annual and seasonal variability in seedbed temperature and water for early plant establishment (Grubb, 1977; Hardegree et al., 2013; Peters, 2000). Our understanding of this variability and knowledge of species-specific responses to water and temperature stress can help us in choosing suitable plant materials and may yield useful strategies for decisions about seedbed preparation, seeding rate, and planting date (Allen et al., 2000; Call and Roundy, 1991; Hardegree et al., 2011).

Hydrothermal germination models have been widely used to characterize the ecophysiological response of seed populations

Published in Crop Sci. 55:2276–2290 (2015).
doi: 10.2135/cropsci2014.10.0703

and to predict the time course of germination under field conditions of seedbed microclimate (Batlla and Benech-Arnold 2003; Bauer et al., 1998; Boddy et al., 2012; Finch-Savage and Phelps, 1993; Finch-Savage et al., 1998; Hardegree et al., 2003, 2013; Meyer and Allen, 2009; Wang et al., 2005). In this modeling approach, cumulative germination rate is measured under a range of constant water potential (ψ) and temperature (T) conditions in the laboratory. Field response is then inferred by assuming constant environmental conditions during a given hour in the field and summing estimated progress toward germination for each hour after planting until germination is predicted to occur (Hardegree et al., 1999; Phelps and Finch-Savage, 1997; Roundy and Biedenbender, 1996).

The probit hydrothermal model is the most common model used to predict germination rate as a function of ψ and T in the field. This model, first characterized by Gummerson (1986) for the suboptimal temperature range, has a number of inherent shape assumptions including a constant base temperature (T_b) and hydrothermal time (θ_{HT}), and a normal distribution of base water potentials (ψ_b) for all seeds within a given population. Alvarado and Bradford (2002) modified the Gummerson model to explain supraoptimal temperature response by hypothesizing a shift in mean ψ_b between the optimal temperature (T_o) and the upper temperature limit for germination. Rowse and Finch-Savage (2003) offered an alternative modification of the Gummerson model at supraoptimal temperatures that explained curvilinearity in thermal response near T_o by linear changes in mean ψ_b above a deviation temperature (T_d). The probit function in these models refers to the optimization of estimates of ψ_b that are assumed to be normally distributed within a population for a given value of T (Alvarado and Bradford, 2002; Gummerson, 1986; Rowse and Finch Savage, 2003).

Hardegree (2006 a,b) and Hardegree and Winstral (2006) tested a variety of thermal germination models and concluded that cumulative germination response could be accurately predicted for a range of field conditions using models that did not require a priori assumptions about model shape parameters. Hardegree et al. (2003, 2013) have described similar regression and statistical-gridding approaches for estimating hydrothermal germination response that optimize model fit without imposing any assumptions about inherent model shape. In this study, we evaluate model shape assumptions for the probit hydrothermal model proposed by Rowse and Finch-Savage (2003) and compare residual model error relative to the regression and statistical-gridding models proposed by Hardegree et al. (2003, 2013). Our objectives were to characterize the magnitude of model error and incidence of bias as a function of T and ψ and to assess the relative impact of these model errors under simulated conditions of soil temperature and water availability in the field.

MATERIALS AND METHODS

Cumulative germination response was assessed over the temperature range of 3 to 36°C and the water potential range of 0 to −2.5 MPa for two seedlots of cheatgrass (*Bromus tectorum*; Kuna and Orchard accessions), four seedlots of bluebunch wheatgrass (*Pseudoroegneria spicata*; MOPX and P4 accessions and two commercial seedlots), three seedlots of bottlebrush squirreltail (*Elymus elymoides*; GV accession and two commercial seedlots), one seedlot of big squirreltail (*Elymus multisetus*; SH accession), and one commercial seedlot each of Sandberg bluegrass (*Poa secunda*), thickspike wheatgrass (*Elymus lanceolatus*), and Idaho fescue (*Festuca idahoensis*). The origins and provenance of these seedlots were previously reported by Hardegree et al. (2013). Detailed procedures for temperature and water potential control, treatment variability and replication, methods for germination detection and seed removal, fungicide treatment, and data-processing are as described by Hardegree et al. (2003).

Cumulative germination percentage as a function of time was calculated for each combination of seedlot, temperature, and water potential for each day of the experiment. Cumulative germination percentage for each day was scaled to a range of 0 to 100% by dividing by the maximum germination percentage (G_m) among chamber-replicate samples following Gummerson (1986). Seed populations were then partitioned into subpopulations (G) on the basis of relative germination rate (Garcia-Huidobro et al., 1982a). Days required to achieve 5 to 95% germination, in 5% increments, were calculated for each treatment by interpolation from the cumulative-germination curves (Covell et al., 1986). Germination rate (R) was calculated as the reciprocal of germination time for each value of G. Daily germination rates were divided by 24 to obtain hourly rate estimates for a given combination of subpopulation, temperature, and water potential (Hardegree and Van Vactor, 2000).

Probit Optimization Model

Hydrothermal model coefficients were estimated for both the sub- and supraoptimal temperature range following a modification of the procedure outlined by Rowse and Finch-Savage (2003). We selected this methodology over that proposed by Alvarado and Bradford (2002) because of observed curvilinearity in thermal germination rate near T_o across most seedlots and subpopulations evaluated in this study (Bloomberg et al., 2009).

T_b was first estimated for all subpopulation/water-potential treatment combinations by extrapolation of a linear model relating R and T (Grundy et al., 2000; Gummerson, 1986; Roman et al., 1999). T_b estimates were similar across subpopulation and water-potential treatment combinations and were averaged to obtain a single seedlot-specific value.

The following probit optimization (PO) procedure was used to estimate mean base water potential [$\psi_b(50)$] and the standard deviation of $\psi_b(50)$ ($\sigma_{\psi b}$) as a function of T. The hydrotime equation of Gummerson (1986) was rearranged to express $\psi_b(G)$ as a function of hydrotime (θ_H), ψ, and germination time as a function of subpopulation [$t(G)$]:

$$\psi_b(G) = \psi - \theta_H t(G)^{-1} \quad [1]$$

Assuming ψ_b was normally distributed among subpopulations, θ_H was iteratively varied in Eq. [1] and Probit(G) plotted as a

function of $\psi_b(G)$ for each thermal regime. The optimal value for θ_H for each temperature was determined as that associated with the lowest coefficient of determination (r^2) for the regression of Probit(G) as a function of $\psi_b(G)$. $\psi_b(50)$ and $\sigma_{\psi b}$ were derived by calculation of the value at which Probit(G) = 0, and the inverse slope of the regression curve, respectively (Bloomberg et al., 2009; Christensen et al., 1996; Kebreab and Murdoch, 1999; Rowse and Finch-Savage, 2003). $\psi_b(50)$ was then plotted as a function of temperature and sub-T_d and supra-T_d thermal regimes identified by visual inspection following the procedure of Rowse and Finch-Savage (2003).

All seedlots had increasing (less negative) estimates of $\psi_b(50)$ as a function of T at supraoptimal temperatures. At suboptimal temperatures, only three seedlots appeared to have a constant value for $\psi_b(50)$ below T_d, as required by the Rowse and Finch-Savage (2003) model. For these three seedlots, all data in the sub-T_d thermal range were pooled for each seedlot for probit optimization of a single equation for estimating $R(G)$ as a function of T and ψ (Alvarado and Bradford, 2002; Rowse and Finch-Savage, 2003). The hydrothermal equation of Gummerson (1986):

$$\theta_{HT} = \left[\psi - \psi_b(G)\right](T - T_b)t(G) \quad [2]$$

was rearranged to yield the following equation:

$$\psi_b(G) = \psi - \theta_{HT}\left[(T - T_b)t(G)\right]^{-1} \quad [3]$$

Values of θ_{HT} were iteratively tested in Eq. [3] and Probit(G) plotted as a function of $\psi_b(G)$ to obtain the regression equation with the highest value for r^2. This procedure yielded the following equation for estimating $\psi_b(G)$:

$$\psi_b(G) = \text{Probit}(G)\sigma_{\psi b} + \psi_b(50) \quad [4]$$

where $\sigma_{\psi b}$, the standard deviation of $\psi_b(G)$, was derived from the inverse slope of the optimized probit regression. Substituting Eq. [4] into Eq. [2] yielded the following equation for estimating suboptimal $R(G)$ as a function of T and ψ at temperatures below T_d:

$$R(G) = t(G)^{-1} = \left[\psi - (\text{Probit}(G)\sigma_{\psi b} + \psi_b(50)\right](T - T_b)\theta_{HT}^{-1} \quad [5]$$

Explicit values for T_d were determined by plotting $\psi_b(50)$ as a linear function of T for the data that appeared by visual inspection to occur in the $T > T_d$ range and solving for the value of T at which supra-T_d and sub-T_d values of $\psi_b(50)$ were equal. The slope (m_1) of the relationship between supra-T_d values of $\psi_b(50)$ and T was used to modify Eq. [5] for estimating $R(G)$ at temperatures above T_d (Bloomberg et al., 2009; Rowse and Finch-Savage, 2003):

$$R(G) = t(G)^{-1} = \left\{\psi - \left[\text{Probit}(G)\sigma_{\psi b} + \psi_b(50) + m_1(T - T_d)\right]\right\} \times (T - T_b)\theta_{HT}^{-1} \quad [6]$$

The other ten seedlots appeared to have $\psi_b(50)$ values that increased with decreasing T in the suboptimal range (Kebreab and Murdoch, 1999). The slope of the relationship between $\psi_b(50)$ and T was also calculated for the suboptimal temperature range (m_2) and a similar equation used to estimate suboptimal $R(G)$ for these seedlots according to the equation:

$$R(G) = t(G)^{-1} = \left\{\psi - \left[\text{Probit}(G)\sigma_{\psi b} + \psi_b(50) + m_2(T - T_d)\right]\right\} \times (T - T_b)\theta_{HT}^{-1} \quad [7]$$

The Rowse and Finch-Savage (2003) model uses the sub-T_d value for $\psi_b(50)$ as the constant baseline from which shifts in $\psi_b(50)$ are estimated for the supra-T_d temperature range, and assumes that $\sigma_{\psi b}$ is constant at all temperatures. For the seedlots that exhibited an upward shift in $\psi_b(50)$ at both sub- and supraoptimal temperatures, the minimum value for $\psi_b(50)$ as a function of T was used as the baseline from which deviations in $\psi_b(50)$ were calculated. Values for $\sigma_{\psi b}$ were relatively constant as a function of temperature, as determined during the procedure to develop Eq. [4] for alternative temperature regimes. We used the mean value for $\sigma_{\psi b}$ as the population estimate of this parameter in both Eq. [6] and Eq. [7] for each seedlot.

The previous procedure for determining the optimal value for θ_{HT} could not be determined with probit optimization for seedlots that had a shift in $\psi_b(50)$ at both sub- and supraoptimal temperatures. Under the assumption that θ_{HT} was constant for all seeds in the population, this variable was iteratively tested for all sub-T_d data using Eq. [7] and all supra-T_d data using Eq. [6]. The optimal value for θ_{HT} was determined to be that value for which the relationship between measured and predicted germination rates, across all subpopulations and hydrothermal treatments, yielded a slope equal to 1 when further constrained to pass through the origin. Negative estimates of predicted germination rate were first set to zero before conducting the correlation analysis.

Initial analysis of the three species exhibiting a constant $\psi_b(50)$ at sub-T_d temperature made the assumption that associated values of θ_{HT} and $\sigma_{\psi b}$ were also suitable for predictions of germination rate in the supra-T_d temperature range. We reanalyzed these seedlots using the same procedure as for the other 10 seedlots to estimate an overall optimal value for θ_{HT} and an average value of $\sigma_{\psi b}$ across the full thermal range. We retained the assumption, however, of a constant value for sub-T_d $\psi_b(50)$ ($m_2 = 0$) in Eq. [7] for these seedlots. This procedure effectively lowered the optimized population estimate of θ_{HT}, but resulted in better overall model fit, so we used the latter procedure for subsequent analyses of residual model error.

Optimized Regression Model

An optimized regression (REG) model was developed from the pooled germination data for each subpopulation of each seedlot to estimate $R(G)$ as a function of T and ψ. This modeling approach was described by Hardegree et al. (2003), but in this study was applied to an additional 7 seedlots. Alternative regression equations were surveyed by parameterizing three dimensional datasets [X = T, Y = ψ, Z = $R(G)$] using the TableCurve3D program (Jandel Scientific). Alternative regression models were screened for best data fit on the basis of coefficient of determination (r^2) values. The nonlinear Lorentzian function (TableCurve Eq. [2024]) used by Hardegree et al. (2003) provided relatively good model fit across seedlots and subpopulations. This model was of the form:

$$R(G) = t(G)^{-1} = a + \frac{b}{1+\left(\frac{T-c}{d}\right)^2} + \frac{e}{1+\left(\frac{\psi-f}{g}\right)^2} + \frac{h}{\left(1+\left(\frac{T-c}{d}\right)^2\right)\left(1+\left(\frac{\psi-f}{g}\right)^2\right)} \quad [8]$$

where $R(G)$ is the subpopulation-specific germination rate (d^{-1}), $t(G)$ is subpopulation-specific germination time (d), and a–f are seedlot and subpopulation-specific model coefficients. The optimized-regression procedure could not resolve equations for slow-germinating subpopulations with an insufficient data density for modeling.

Statistical Gridding Model

A hydrothermal germination rate model was developed for each subpopulation of each seedlot using a modification of the statistical-gridding (SG) procedure described by Hardegree and Winstral (2006) for thermal germination models. Instead of plotting R as a function of G and T, we plotted $R(G)$ as a function of T and ψ for each seedlot and subpopulation using the methodology described by Hardegree et al. (2013). This procedure uses algorithms similar to topographic mapping programs to produce a response surface that triangulates rate estimates by direct interpolation from treatment data (Hardegree et al., 2013).

Evaluation of Model Residual Error

To maximize comparability across all modeling procedures and seedlots, analysis of model fit was constrained to the 5 to 50% subpopulation range that was included in all REG models for all species. Residual model error (predicted-measured) for germination rate was calculated for each treatment combination of G, T and ψ. A root mean square error (RMSE) term for all model data, and for the model data in the common 5 to 50% subpopulation range, were calculated for direct comparison among species and subpopulations for overall model fit.

We evaluated relative model fit by calculating model residual errors for all combinations of seedlot, G, T, and ψ and plotting error responses averaged for each seedlot by the variables G, T, and ψ. Average residual errors for all seedlots were plotted for each variable and a quadratic equation was used to estimate mean error as a function of G, T, and ψ across all seedlots. Ninety-five percent confidence and predictive bands were estimated to evaluate systematic model errors as a function of individual model variables.

Residual model error was also evaluated by correlation analysis of observed and modeled germination rate for each species and model. This analysis was also restricted to the 0 to 50% subpopulation range to facilitate comparisons across seedlots, as the *P. sandbergii* seedlot had insufficient data to parameterize the regression model in the 55 to 95% subpopulation range.

Field Simulation of Model Differences

Hardegree et al. (2013) used a 44-yr simulation of T and ψ at seeding depth to evaluate these same seedlots under typical conditions that might be experienced in the field. We used this same simulated field record to compare potential germination response among the three models used in the current study. This microclimatic simulation was previously validated for a field soil in southern Idaho (Tindahay sandy-loam; sandy, mixed mesic, Xeric Torriorthent) using the simultaneous heat and water (SHAW) model as described by Flerchinger et al. (2012). Model output consisted of hourly temperature and water potential at 2-cm depth for the period October 1, 1961, through September 30, 2005. Seeding decisions in this region are typically implemented in late October, and environmental effects on establishment are typically interpreted relative to the hydrologic year (October through September) rather than the calendar year. Hourly T and ψ estimates from the field simulation were used to estimate R for each combination of seedlot, subpopulation, and hydrothermal model. Per-hour germination rate estimates represent the fractional progress toward germination for a given subpopulation during a given hour (Hardegree, 2006b). Germination time for a given subpopulation can be estimated when the sum of hourly post-planting germination rates becomes equal to 1 (Roundy and Biedenbender, 1996). The annual rate sum represents the number of times a given subpopulation might have germinated in a given year if identical seeds were replanted after every germination event. The cumulative rate-sum, therefore, is a site- and year-specific index of relative favorability of seedbed microclimate for germination (Hardegree et al., 2013). Hourly rate estimates were aggregated to provide a rate-sum estimate for each hydrologic year of the field simulation.

An annual rate-sum value for all subpopulations and simulation years was calculated for each seedlot and model type. We regressed PO, REG, and SG-model rate-sum values for the 5 to 50% subpopulations of each seedlot across all simulation years and used the slope and r^2 values to estimate relative model fit under field-variable conditions of temperature and moisture.

RESULTS

Cumulative germination curves for six combinations of T and ψ are shown in Fig. 1 for a general visualization of relative water stress and temperature effects across seedlots. Cheatgrass (*B. tectorum*) consistently exhibited more rapid germination across all hydrothermal regimes for the more rapid germinating subpopulations, but with a drop-off in relative rate for later germinating seeds.

Relative model shapes of PO, REG, and SG models are shown in Fig. 2 for slow (*F. idahoensis*, commercial), medium (*E. elymoides*, GV), and rapid-germinating (*B. tectorum*, Kuna) seedlots for the 25% subpopulation. The PO model was specifically constrained to a constant T_b, but the REG model was not so constrained (Fig. 2). Analysis of model error, however, does not include treatments near T_b as the analysis was limited to the measured thermal range of 3 to 36°C. Lower temperature limits from the SG model do not converge on a single T_b as this model was parameterized to include only measured rate data, and treatments with no germination were set to zero rather than extrapolated from adjacent model points. The SG model consists of a simple planar interpolation from measured germination rates and so represents the actual data distribution (Fig. 2).

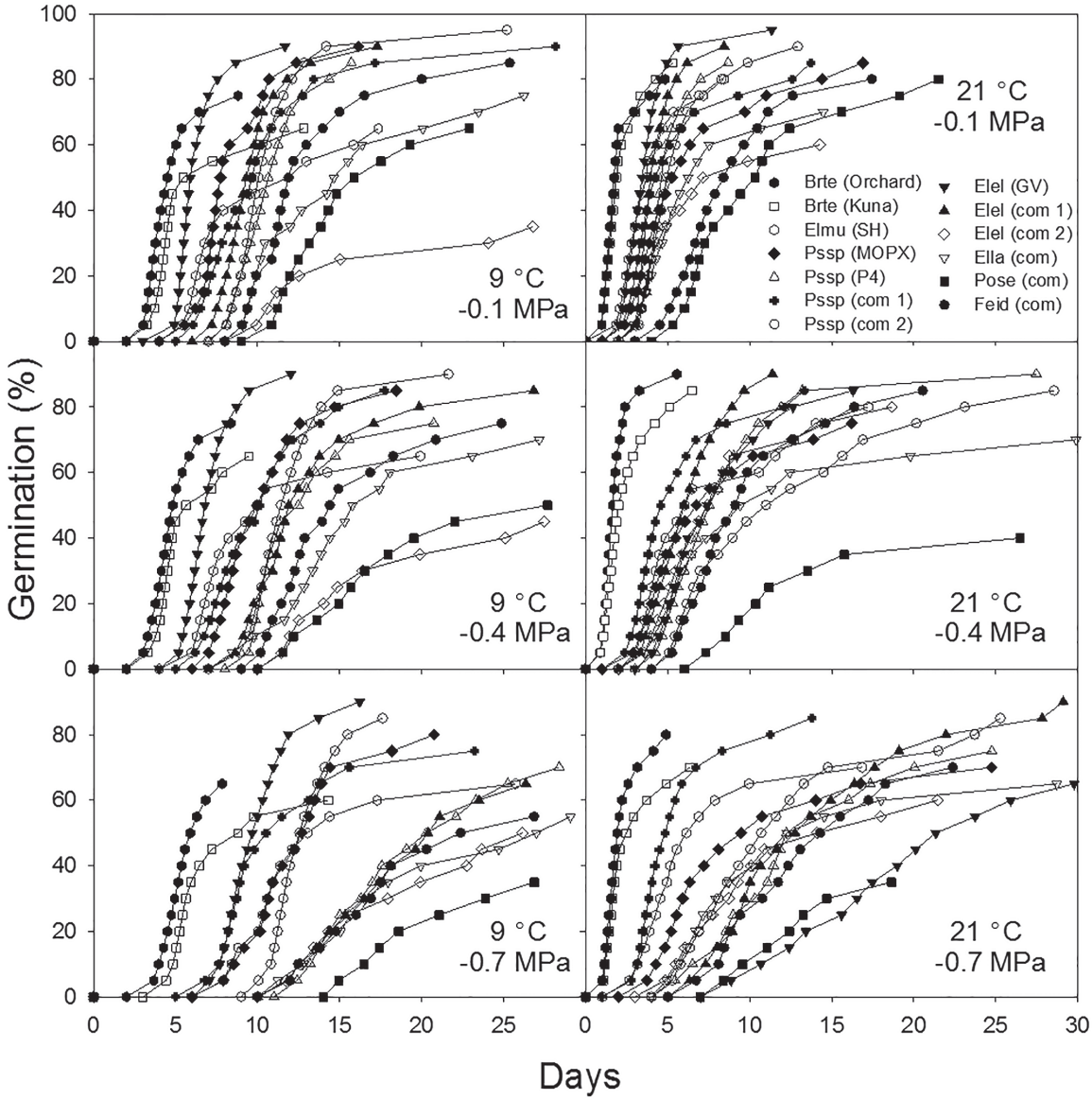

Figure 1. Cumulative germination response for relative comparison of all seedlots at two temperatures (9 and 21°C) and three water potentials (−0.1, −0.4 and −0.7 MPa). Brte, *Bromus tectorum*; com, commercial; Elel, *Elymus elymoides*; Ella, *Elymus lanceolatus*; Elmu, *Elymus multisetus*, Feid, *Festuca idahoensis*; Pose, *Poa secunda*; Pssp, *Pseudoroegneria spicata*.

Probit model parameters are shown in Table 1 for all seedlots. Values for $\psi_b(50)$ as a function of temperature, derived by probit optimization of Eq. [4], appeared to be constant in the suboptimal temperature range for only three of the seedlots tested (Fig. 3). Estimates of $\sigma_{\psi b}$ were relatively consistent across thermal regimes for a given seedlot (Fig. 4) so were averaged for a single value per seedlot (Table 1). Overall variability in the distribution of $\psi_b(G)$ as a function of Probit(G) was indicated by r^2 values ranging from 0.74 to 0.91 with an average across seedlots of 0.83.

The PO and SG models were capable of modeling the entire subpopulation range regardless of relative data density as a function of T and ψ treatments. To facilitate comparisons among different models, only treatment data in the subpopulation range accessible to the REG model were used in PO and SG model development. Table 2 lists the subpopulation range for each seedlot used for model comparisons. Table 2 also provides an overall RMSE value for each seedlot and model for both the full subpopulation range of a given seedlot and for measurements only in the 5 to 50% subpopulation range. Root mean square error values are scale dependent, so relative comparisons of overall model error can only be made among models within a given seedlot. Table 2, however, notes that average RMSE for the REG model is approximately 60% of the error rate for the PO model, and the SG model error is an order of magnitude lower than the other models.

Analysis of residual model error as a function of G, T, and ψ revealed systematic error patterns in PO and REG model estimates of germination rate (Fig. 5, Fig. 6, Fig. 7). The PO model tended to overestimate rate for the faster and slower-germinating subpopulations, and underestimate rate for the mid-range of subpopulations (Fig.

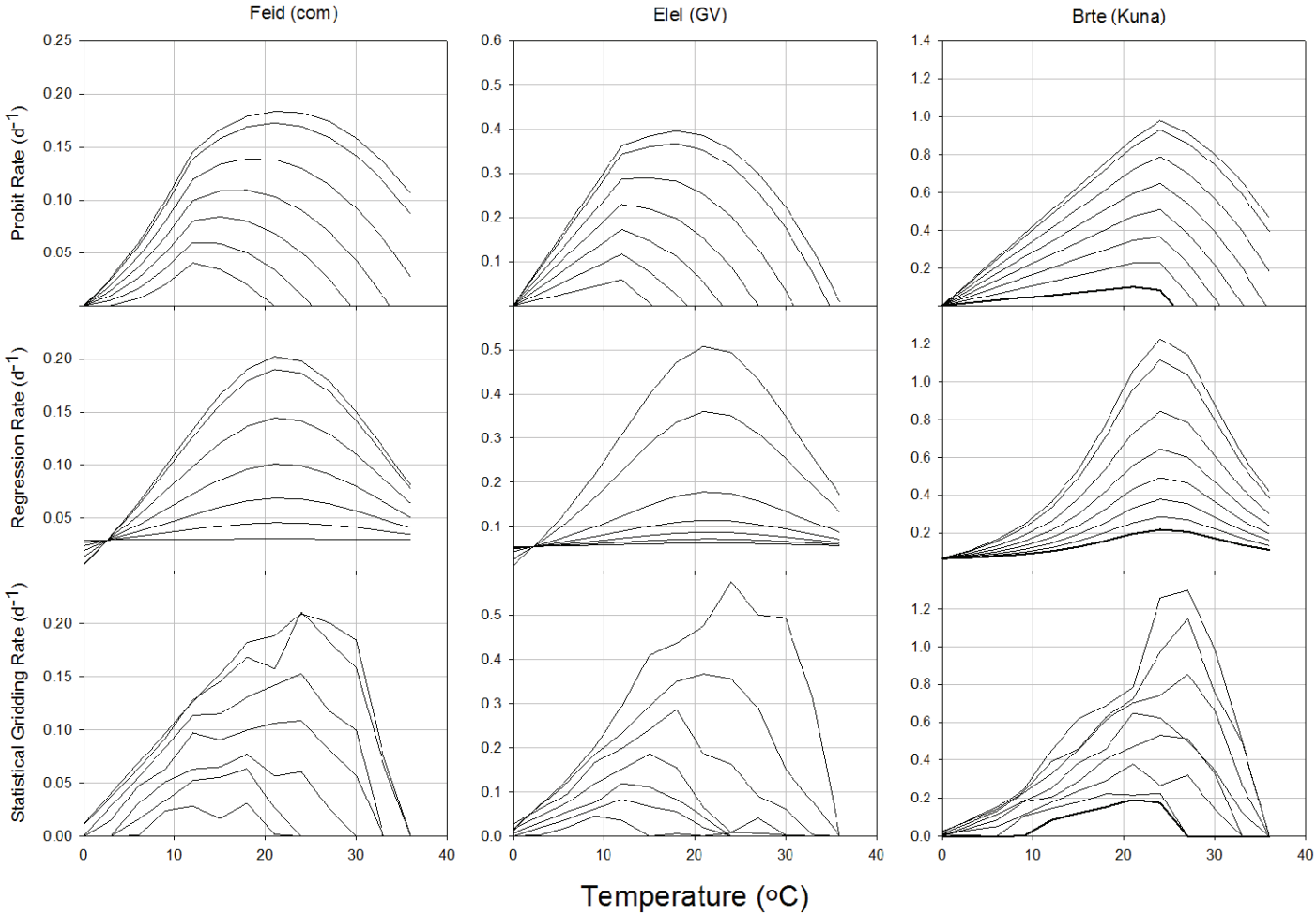

Figure 2. Model shapes for low (*Festuca idahoensis* [Feid], commercial [com]), medium (*Elymus elymoides* [Elel], GV), and fast-germinating (*Bromus tectorum* [Brte], Kuna) seeds for probit optimization, optimized regression, and statistical gridding models for the 25% subpopulation. Upper to lower lines represent water potentials of 0, −0.1, −0.4, −0.7, −1.0, −1.3, −1.6, and −1.9 MPa, respectively.

Table 1. Probit hydrothermal model coefficients for Eq. [6] and Eq. [7].

Species†	Seedlot	T_b	T_d	θ_{HT} (at T_d)	$\psi_b(50)$	$\sigma_{\psi b}$	m_1	m_2
Brte	Orchard	−0.09	18.0	49	−2.12	0.788	0.125	−0.044
Brte	Kuna	−0.10	23.4	51	−1.48	0.992	0.118	0
Elmu	SH	−0.02	14.7	70	−1.36	0.604	0.085	0
Pssp	MOPX	−0.02	11.3	77	−1.61	0.463	0.097	−0.057
Pssp	P4	−0.04	12.4	92	−1.52	0.386	0.064	−0.094
Pssp	com‡ 1	−0.02	11.4	132	−2.79	0.621	0.122	−0.092
Pssp	com 2	0.00	11.0	135	−2.16	0.367	0.092	−0.106
Elel	GV	0.00	11.2	63	−1.68	0.348	0.077	0
Elel	com 1	−0.01	14.5	98	−1.50	0.331	0.044	−0.065
Elel	com 2	−0.04	12.0	168	−1.83	0.864	0.067	−0.158
Ella	com	−0.03	12.7	137	−1.81	0.587	0.085	−0.086
Pose	com	−0.01	11.5	148	−1.48	0.486	0.084	−0.151
Feid	com	0.00	12.1	182	−1.83	0.582	0.071	−0.068

† Brte, *Bromus tectorum*; Elel, *Elymus elymoides*; Ella, *Elymus lanceolatus*; Elmu, *Elymus multisetus*, Feid, *Festuca idahoensis*; Pose, *Poa secunda*; Pssp, *Pseudoroegneria spicata*.
‡ com, commercial.

5). Average model error as a function of *G* for REG and SG models was insignificant (data not shown), which was not surprising given that these models were optimized for individual values of *G*. PO models overestimated germination rates in the suboptimal temperature range and underestimated rates in the supra-optimal temperature range except for the highest temperature treatments (Fig. 6). This general error pattern is similar to that shown by Hardegree (2006a). The PO model also tended to overestimate germination rate at lower water potentials and

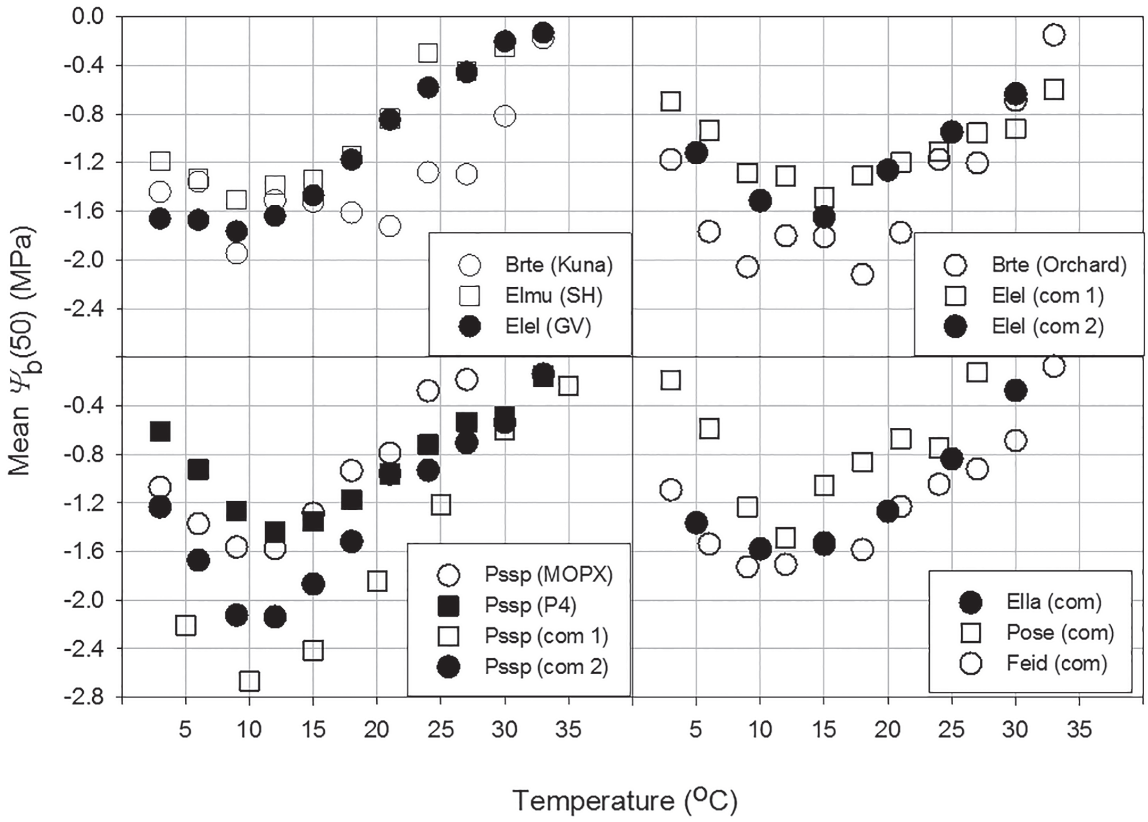

Figure 3. Distribution of mean base water potential [$\psi_b(50)$] as a function of temperature (T) for seedlots determined to have a relatively constant value below deviation temperature (T_d) (Brte, Kuna; Elmu, SH; and Elel, GV) and those determined to vary below T_d. Specific values for $\psi_b(50)$ at T_d are listed in Table 1. Brte, *Bromus tectorum*; com, commercial; Elel, *Elymus elymoides*; Ella, *Elymus lanceolatus*; Elmu, *Elymus multisetus*, Feid, *Festuca idahoensis*; Pose, *Poa secunda*; Pssp, *Pseudoroegneria spicata*.

underestimate rate in the highest water potential treatments (Fig. 7). The REG model tended to overestimate rate only in the highest temperature treatments (Fig. 6) but also overestimated rate over most of the lower water potential range (Fig. 7).

Correlation analysis is another option for assessing relative model error. Figure 8 shows the relationship between observed and predicted germination rate for all combinations of temperature and water potential treatments for the 5 to 50% subpopulations of three representative seedlots. The slope and r^2 values for observed vs. predicted correlations for all seedlots and models are shown in Table 3. These regressions were constrained to pass through the origin, and treatments with observed germination rates = 0 were excluded. All the slope values were less than 1, indicating that models tended to underestimate rate across all treatments. Values of r^2 were lowest for PO and highest for SG models and tended to be lower for species germinating at intermediate rates compared with their slower or faster germinating counterparts.

Laboratory test conditions included broader temperature and water potential ranges than typically relevant for field conditions of germination and emergence in the Great Basin (Hardegree et al., 2003). The relative accuracy of field predictions, therefore, may only be responsive to a subset of treatment conditions and associated model errors from the laboratory experiment. Annual rate sums for each seedlot were calculated for each subpopulation for each year of the field simulation to estimate relative model error under a more realistic set of potential treatment conditions. The 5 to 50% subpopulation range shows relatively consistent patterns among models (Fig. 9, Table 4). The slope of SG vs. REG rate sum regressions are consistently greater than 1, indicating a general overestimation of REG-derived germination rate for all seedlots relative to the SG model (data not plotted for all species but regression results are summarized in Table 4). This difference in REG rate sum estimates relative to the SG model ranged from 4 to 32% among species, with an average of 11% (Table 4). The PO model also tended to overestimate annual rate sums relative to the SG model by 13% across all species, although this model slightly underestimated annual rate sums by 1 to 3% in 4 of the 13 seedlots (Fig. 9, Table 4). A similar comparison of PO and REG models was inconclusive, with higher variability among seedlots in regression slope, although r^2 values were relatively high for all rate sum comparisons (Table 4).

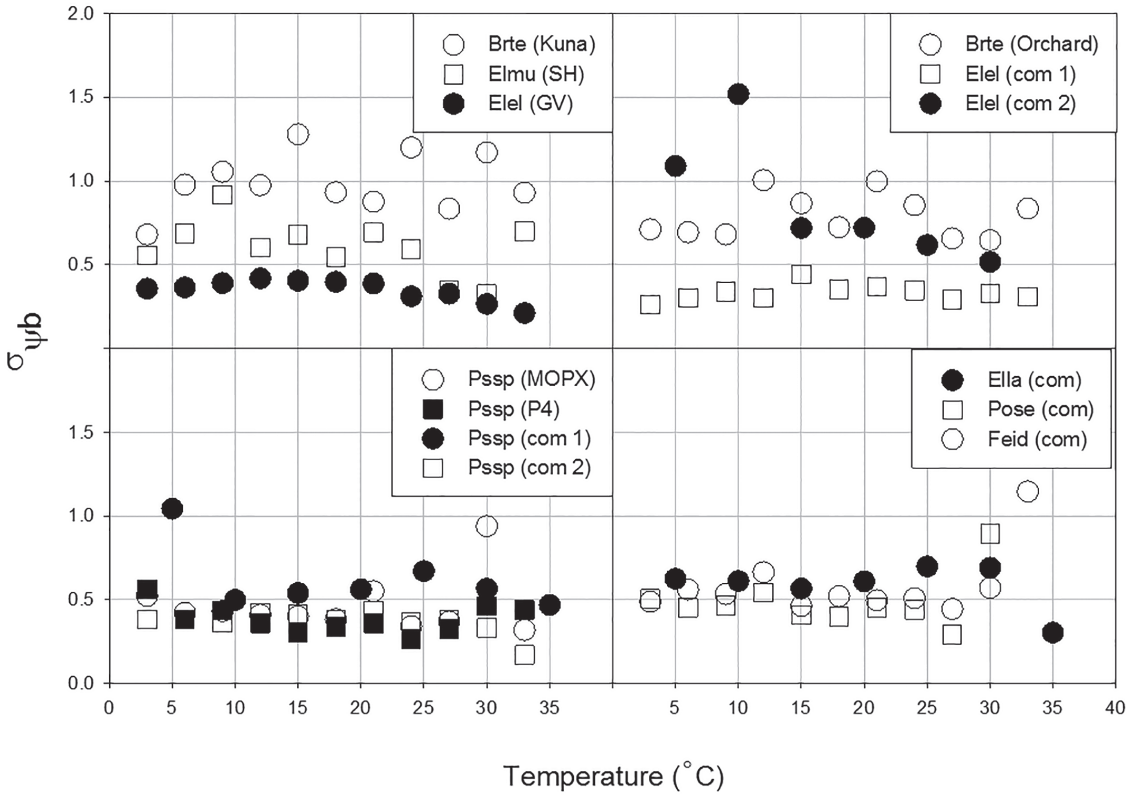

Figure 4. Distribution of $\sigma_{\psi b}$, the standard deviation of $\psi_b(G)$, as a function of temperature for all tested seedlots. Specific average values used in the probit optimization model are listed in Table 1.

Table 2. Model root mean square error (RMSE) for all seedlots for the full range of subpopulations modeled and for the 5 to 50% subpopulations to facilitate comparisons across seedlots. PO, probit optimization; REG, optimized regression; SG, statistical gridding.

Species†	Seedlot	Full model range	Full-range PO model RMSE	Full-range REG model RMSE	Full-range SG model RMSE	5–50% PO model RMSE	5–50% REG model RMSE	5–50% SG model RMSE
Brte	Orchard	5–75	0.115	0.063	0.005	0.120	0.066	0.005
Brte	Kuna	5–65	0.096	0.061	0.005	0.095	0.060	0.004
Elmu	SH	5–70	0.056	0.029	0.005	0.056	0.032	0.005
Pssp	MOPX	5–90	0.037	0.023	0.002	0.042	0.028	0.002
Pssp	P4	5–85	0.030	0.020	0.002	0.031	0.022	0.002
Pssp	com‡ 1	5–55	0.034	0.026	0.003	0.035	0.026	0.004
Pssp	com 2	5–90	0.023	0.017	0.002	0.025	0.019	0.002
Elel	GV	5–90	0.050	0.034	0.002	0.054	0.038	0.003
Elel	com 1	5–90	0.022	0.013	0.002	0.022	0.014	0.002
Elel	com 2	5–55	0.025	0.017	0.002	0.025	0.016	0.002
Ella	com	5–70	0.019	0.011	0.001	0.020	0.012	0.001
Pose	com	5–50	0.017	0.010	0.002	0.017	0.010	0.002
Feid	com	5–85	0.014	0.010	0.001	0.014	0.010	0.001
		average	0.041	0.026	0.003	0.043	0.027	0.003

† Brte, *Bromus tectorum*; Elel, *Elymus elymoides*; Ella, *Elymus lanceolatus*; Elmu, *Elymus multisetus*, Feid, *Festuca idahoensis*; Pose, *Poa secunda*; Pssp, *Pseudoroegneria spicata*.

‡ com, commercial.

DISCUSSION

Current methodology for the probit hydrothermal model evolved from key earlier work describing within-population variability in thermal response to temperature (Garcia-Huidobro et al., 1982a,b), characterization of normally distributed model parameters (Covell et al., 1986; Ellis et al., 1986, 1987), and incorporation of water potential and temperature interactions and response patterns (Gummerson, 1986). Subsequent refinements have improved general model fit and enhanced our physiological understanding of hydrothermal response, particularly in the supraoptimal temperature range (Bloomberg et al., 2009; Alvarado and Bradford, 2002; Rowse and Finch-Savage, 2003). Probit hydrothermal models, however,

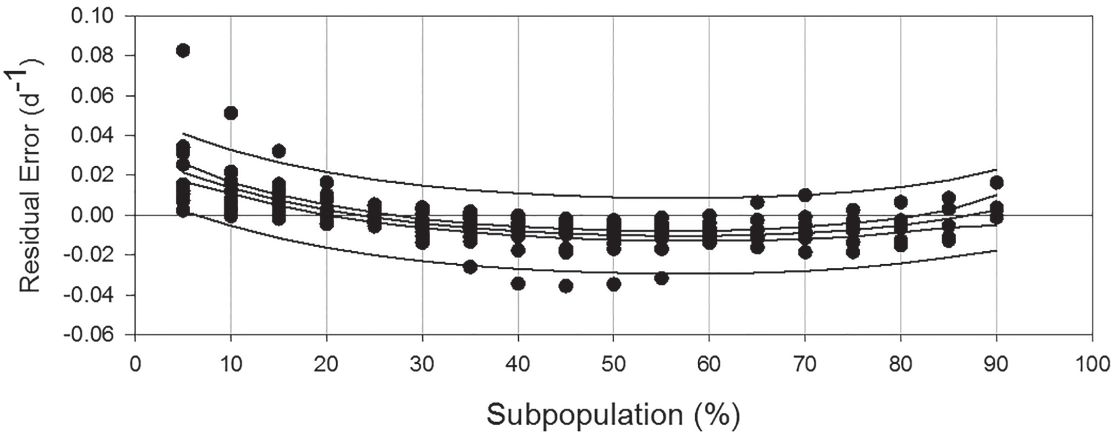

Figure 5. Average residual probit optimization model error across all temperature and water potential values for all seedlots as a function of germination percentage (*G*) (middle lines). The 95% confidence (inner lines) and prediction (outer lines) bands were derived from a quadratic regression model. Each data point represents the average model error for a single seedlot at a given value of *G*.

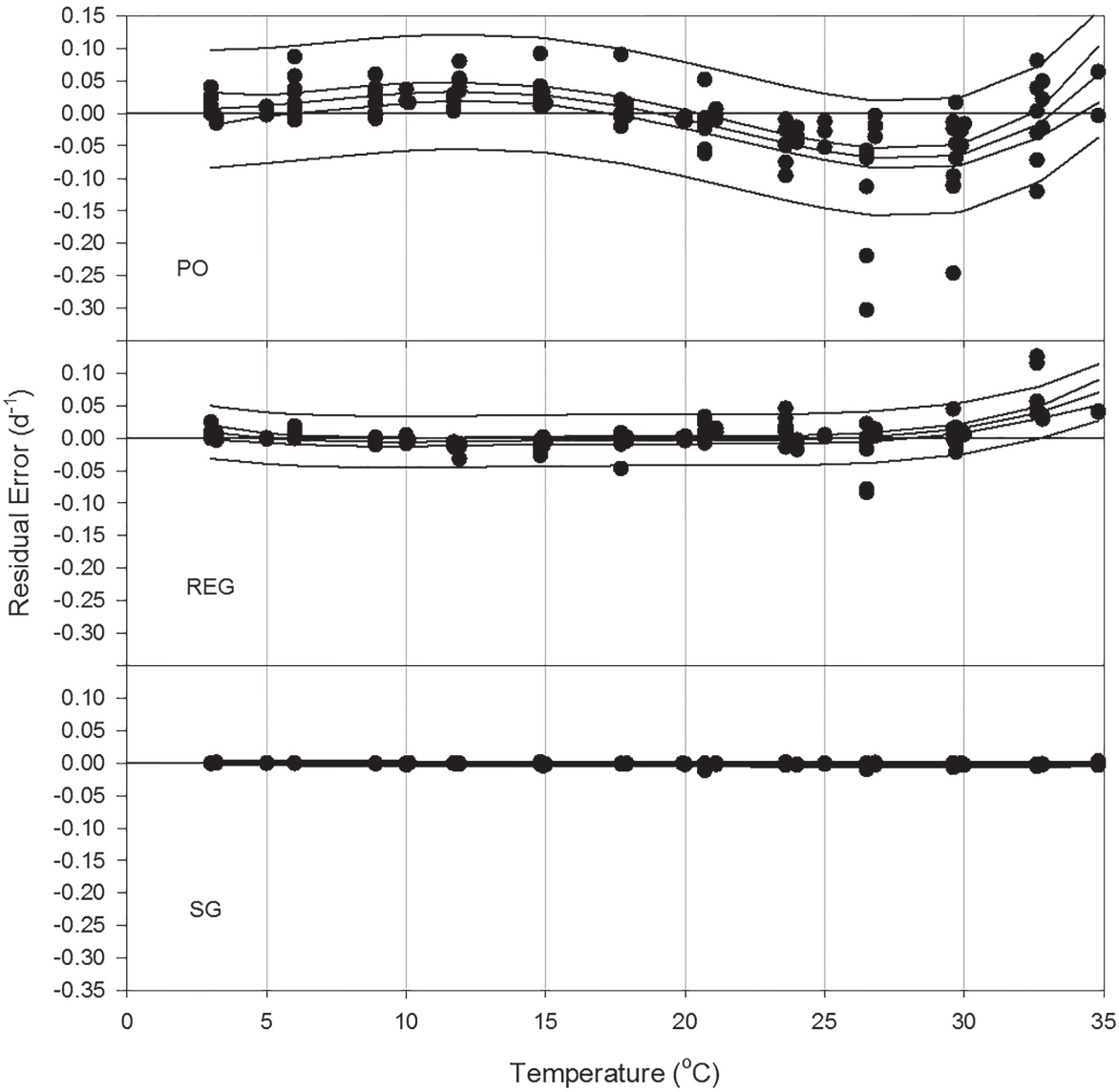

Figure 6. Average residual model error across all water potential and germination percentage values for all seedlots as a function of temperature (*T*) (middle lines). The 95% confidence (inner lines) and prediction (outer lines) bands were derived from a quadratic regression model. Each data point represents the average model error for a single seedlot at a given value of *T*. PO, probit optimization; REG, optimized regression; SG, statistical gridding.

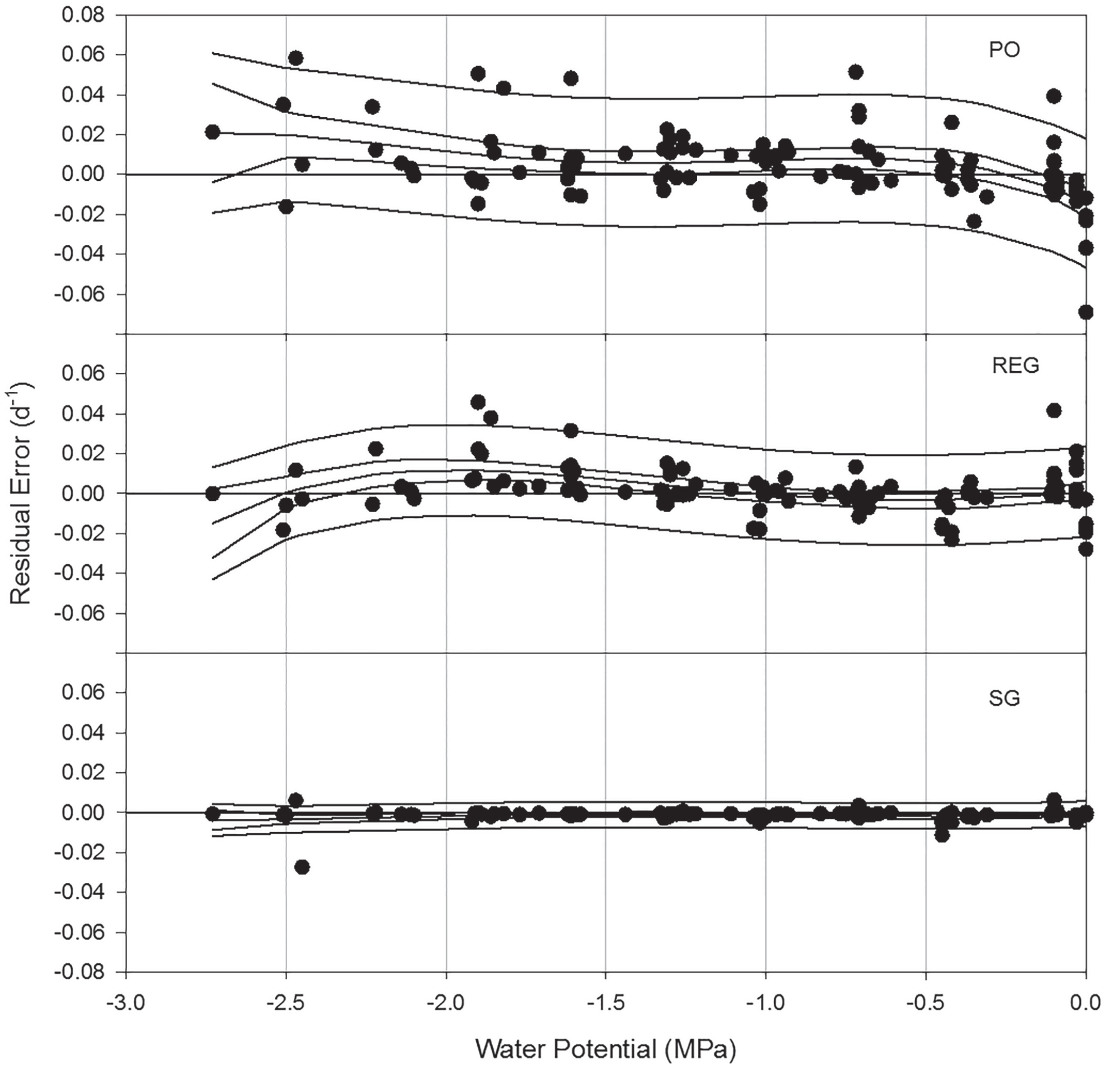

Figure 7. Average residual model error across all temperature and germination percentage values for all seedlots as a function of water potential (ψ) (middle lines). The 95% confidence (inner lines) and prediction (outer lines) bands were derived from a quadratic regression model. Each data point represents the average model error for a single seedlot at a given value of ψ. PO, probit optimization; REG, optimized regression; SG, statistical gridding.

require the adoption of multiple model-shape assumptions including commonality of T_b and θ_{HT}, linearity of suboptimal temperature response (constant θ_T[G]), and a normal distribution of ψ_b(G) and θ_T(G). These assumptions allow the modeler to parse individual computational elements of the general model and derive physiologically relevant model coefficients that can be directly compared across seedlots and species (Allen, 2003; Bradford, 1990). The principal benefits of this modeling approach also include consistency of methodology across species and seedlots, generation of numerical coefficients to understand alternative germination syndromes, explicit linkage of model parameters to physiological processes, and relatively tractable computational procedures that linearize population variability and facilitate visualization of key model parameters. The primary drawbacks to this approach are that the procedures for model development are relatively tedious compared with the generic optimization procedures of the REG and SG models, and the PO model demonstrated lower model fit over the entire temperature and water potential range tested (Table 2, Fig. 6, Fig. 7).

If the principal modeling objective is to maximize model fit and, therefore, predictive accuracy for estimating cumulative germination, then wholly empirical REG and SG model formulations may be more desirable (Hardegree et al., 2003, 2013). We used equation discovery to identify a single regression model that fit relatively well across seedlots and subpopulations, but a similar approach could be used to select alternative models optimized at the individual seedlot and subpopulation level. Of the three modeling approaches, optimized regression was the most computationally efficient. The entire procedure consisted of importing T, ψ, and G data into a commercial program for equation discovery and generating a list of optimized regression equations presorted by their r^2 values. Upon selection of a given model, this procedure was also

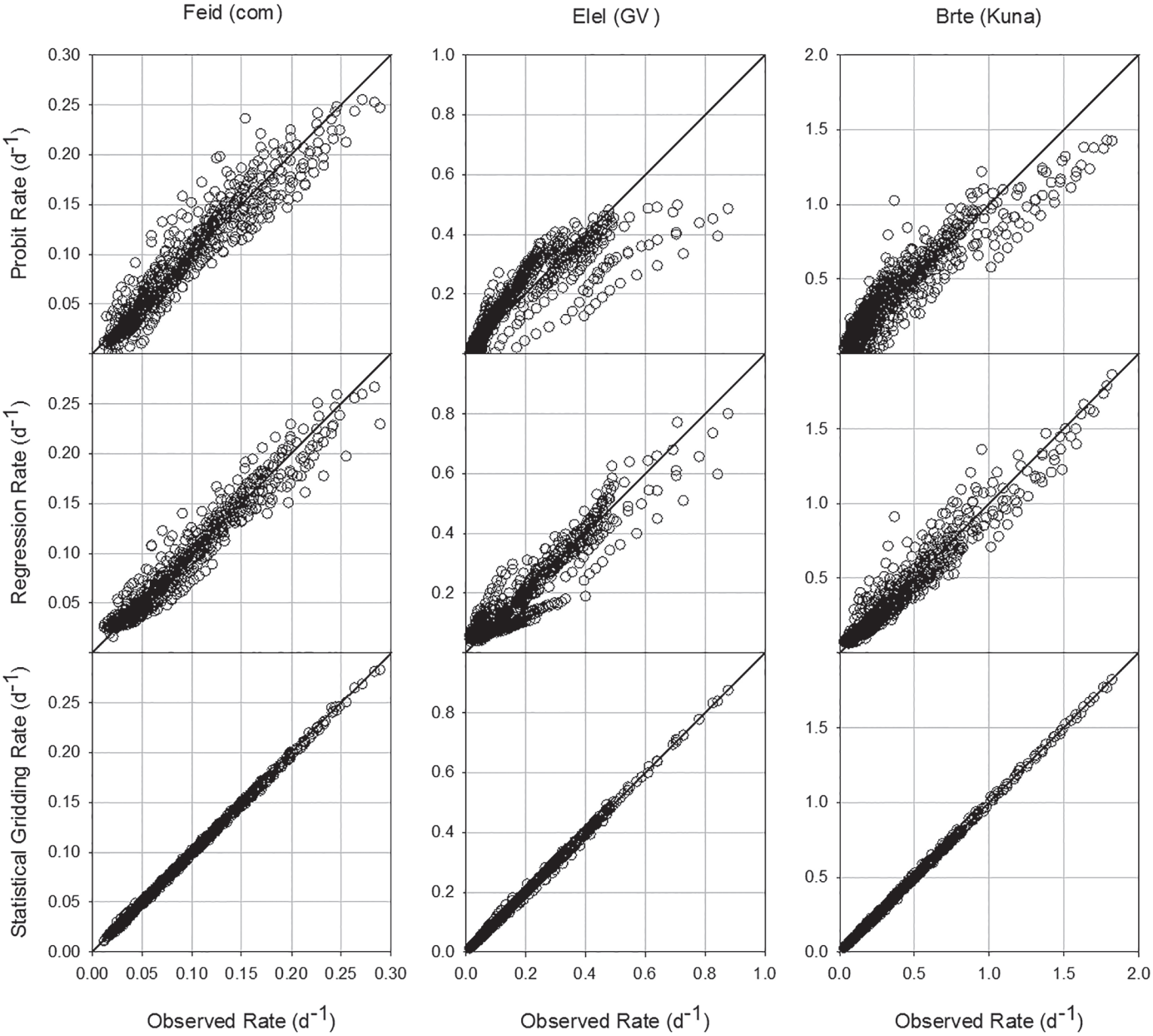

Figure 8. Observed vs. predicted germination rate (*R*) for low (*Festuca idahoensis* [Feid], commercial [com]), medium (*Elymus elymoides* [Elel], GV), and fast-germinating (*Bromus tectorum* [Brte], Kuna) seeds for probit optimization, optimized regression, and statistical gridding models. Model data were only included for the 5 to 50% values of germination percentage (*G*) to facilitate inter-seedlot comparison. Line represents a regression with a slope of 1 and r^2 of 1.00. Actual regression slopes and r^2 values for all seedlots are listed in Table 3.

relatively efficient in estimating germination rate as a single equation applied to the full range of ψ and T conditions within a given subpopulation. The principal drawback for this methodology was the relatively high data density required to resolve accurate model estimates for slower-germinating subpopulations. This limits the applicability of these models, although all seedlots tested produced relatively accurate estimates of germination rate up to the 50% subpopulation, which is a widely used baseline for comparisons among seedlots and species (Brown and Mayer, 1988; Scott et al., 1984). Systematic bias was lower for REG than for PO models and primarily restricted to higher temperatures and lower water potentials (Table 2; Fig. 6, Fig. 7).

The SG model showed significantly lower predictive error than the REG or PO models (Table 2). This is not surprising given that the model was optimized to fit the actual data field with no shape assumptions and associated predictive-model error. Visualization of shape functions (Fig. 2) shows additional differences between the SG, PO, and REG-model estimates. The REG and PO models induce constant values for T_o and T_d, respectively, which are not apparent in the SG data distribution. The PO model and SG data distributions, however, show a clear downward shift in thermal optima at reduced water potential compared with the REG model (Fig. 2). We do not have data to confirm the accuracy of the SG model

Table 3. Slope and coefficient of determination (r^2) values for all seedlots for observed vs. predicted germination rates (see Fig. 8). Regressions were determined for the 5 to 50% subpopulation range to facilitate comparisons across seedlots. REG, optimized regression; SG, statistical gridding.

Species†	Seedlot	Probit model slope	REG model slope	SG model slope	Probit model r^2	REG model r^2	SG model r^2
Brte	Orchard	0.91	0.97	1.00	0.74	0.92	1.00
Brte	Kuna	0.94	0.97	1.00	0.83	0.93	1.00
Elmu	SH	0.89	0.96	0.99	0.67	0.90	0.99
Pssp	MOPX	0.90	0.95	0.99	0.68	0.87	1.00
Pssp	P4	0.96	0.97	1.00	0.79	0.92	1.00
Pssp	com‡ 1	0.90	0.95	0.99	0.72	0.86	1.00
Pssp	com 2	0.92	0.97	0.99	0.77	0.89	1.00
Elel	GV	0.89	0.96	1.00	0.64	0.88	1.00
Elel	com 1	0.98	0.99	0.99	0.92	0.97	1.00
Elel	com 2	0.95	0.97	0.99	0.82	0.93	1.00
Ella	com	0.94	0.98	0.99	0.86	0.94	1.00
Pose	com	0.96	0.98	0.99	0.79	0.90	1.00
Feid	com	0.98	0.98	0.99	0.90	0.94	1.00
	average	0.93	0.97	0.99	0.78	0.91	1.00

† Brte, *Bromus tectorum*; Elel, *Elymus elymoides*; Ella, *Elymus lanceolatus*; Elmu, *Elymus multisetus*, Feid, *Festuca idahoensis*; Pose, *Poa secunda*; Pssp, *Pseudoroegneria spicata*.

‡ com, commercial.

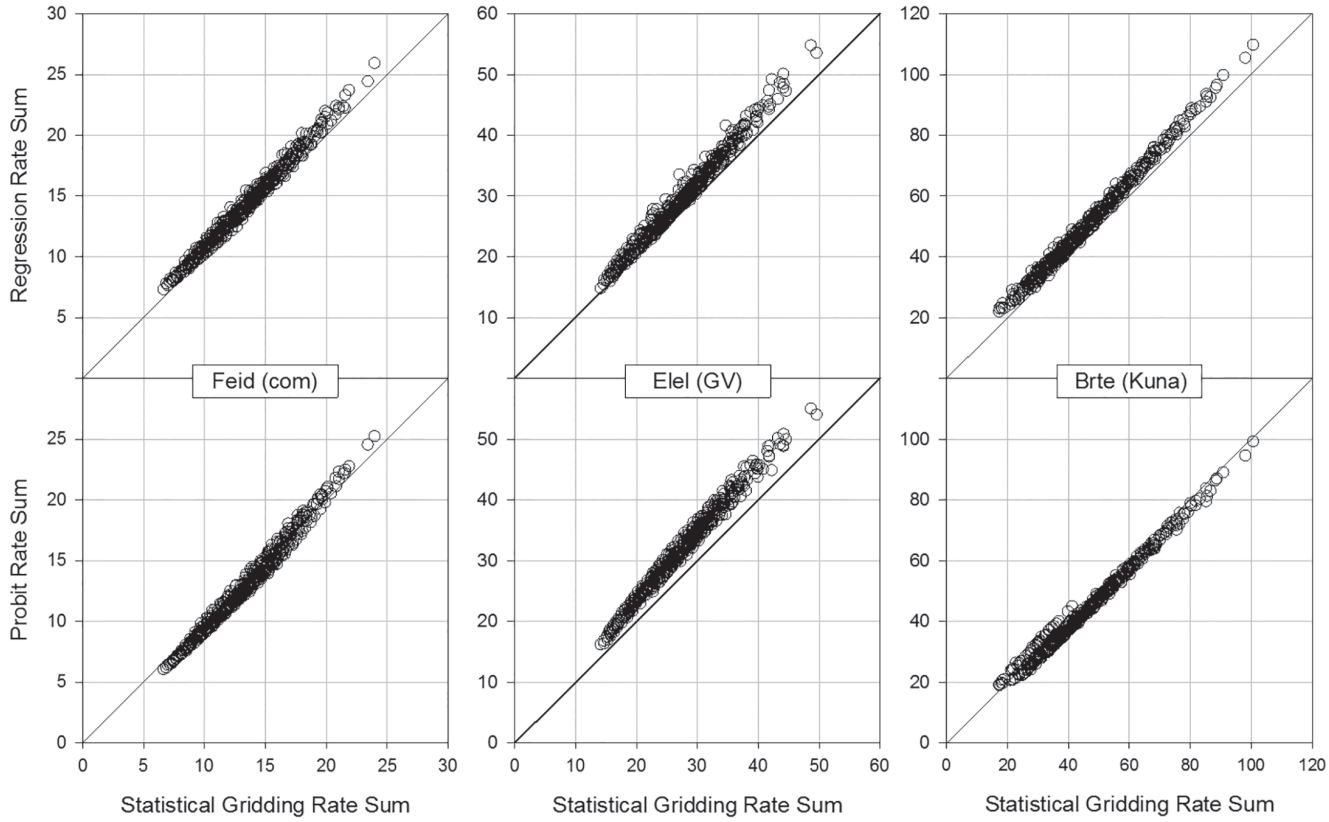

Figure 9. Annual rate-sum comparison for statistical gridding vs. optimized regression and statistical gridding vs. probit optimization models for low (*Festuca idahoensis* [Feid], commercial [com]), medium (*Elymus elymoides* [Elel], GV), and fast-germinating (*Bromus tectorum* [Brte], Kuna) seeds. Model data were only included for the 5 to 50% values of germination percentage (*G*) to facilitate inter-seedlot comparison. Line represents a regression with a slope of 1 and r^2 of 1.00. Actual regression slopes and r^2 values for all seedlots are listed in Table 4.

under field-variable conditions of ψ, but previous studies have validated SG-type models under controlled and replicated conditions of variable temperature (Hardegree, 2006b; Hardegree and Van Vactor, 1999).

Detailed hydrothermal germination studies are often limited in scope to a small number of seedlots (e.g., Dahal and Bradford, 1994; Grundy et al., 2000; Gummerson, 1986; Hardegree et al., 2003; Kebreab and Murdoch, 1999;

Table 4. Slope and coefficient of determination (r^2) values for comparison of annual rate sums for all seedlots and subpopulations and 44-yr modeling period (see Fig. 9). Regressions were determined for the 5 to 50% subpopulation range to facilitate comparisons across seedlots. SG, statistical gridding; Prob, probit optimization; REG, optimized regression.

Species†	Seedlot	SG vs. Prob slope	SG vs. Reg slope	REG vs. Prob slope	SG vs. Prob r^2	SG vs. REG r^2	REG vs. Prob r^2
Brte	Orchard	1.19	1.04	1.14	0.99	0.92	0.95
Brte	Kuna	0.97	1.10	0.88	0.99	0.99	0.98
Elmu	SH	1.19	1.07	1.11	1.00	0.97	0.97
Pssp	MOPX	1.12	1.08	1.03	0.99	0.99	0.96
Pssp	P4	1.12	1.06	1.05	0.99	0.98	0.98
Pssp	com‡ 1	1.37	1.32	1.05	0.93	0.92	0.88
Pssp	com 2	1.07	1.09	0.98	0.98	0.99	0.96
Elel	GV	1.16	1.08	1.08	0.99	0.98	0.96
Elel	com 1	0.99	1.06	0.93	1.00	0.98	0.99
Elel	com 2	1.38	1.23	1.12	0.97	0.99	0.95
Ella	com	1.18	1.12	1.06	0.97	0.99	0.95
Pose	com	0.97	1.11	0.87	0.99	0.99	0.98
Feid	com	0.97	1.06	0.91	0.99	0.99	0.99
	average	1.13	1.11	1.02	0.98	0.98	0.96

† Brte, *Bromus tectorum*; Elel, *Elymus elymoides*; Ella, *Elymus lanceolatus*; Elmu, *Elymus multisetus*, Feid, *Festuca idahoensis*; Pose, *Poa secunda*; Pssp, *Pseudoroegneria spicata*.
‡ com, commercial.

Rowse and Finch-Savage, 2003; Wang et al., 2005). It is relatively difficult to apply such intensive measurement techniques to test the validity of model shape assumptions across multiple seedlots. Large-scale hydrothermal parameter assessment usually involves a severe reduction in the number of temperature and water potential treatments tested or relies on surrogate estimates of main model parameters (Allen et al., 2000; Allen and Meyer, 1998; Cheng and Bradford, 1999; Finch-Savage and Phelps, 1993; Köchy and Tielbörger, 2007). These studies may have insufficient data densities to confirm major shape assumptions, some of which proved invalid in the current study and in some previous studies, particularly those related to the assumption of a constant $\psi_b(50)$ in the suboptimal temperature range (Fig. 3; Kebreab and Murdoch, 1999).

Arnold (1959) noted that the most relevant assessment of model fit should be based on how well the model predicts practical information such as the time taken to germinate in the field. Hardegree et al. (2003, 2013) also suggested that the integration of field-variable germination response provides the most ecologically relevant basis for comparison of species and for identification of alternative germination syndromes. The cumulative rate-sum parameter used to generate the data in Fig. 9 integrates the effective germination response under variable field conditions and is directly proportional to expectations of germination time in the field (Hardegree et al., 2003, 2013). Significant deviations from linearity for model comparisons in Fig. 9 may, therefore, give a more accurate picture of relevant model errors than previous comparisons of model parameters (Table 1) or model fit (Table 2, Fig. 5, Fig. 6, Fig. 7). Figure 9 and Table 4 show relatively high correlations among different models that, on average, deviated from unity by less than 15%. The larger deviations exhibited by some seedlots, however, may alone justify use of wholly empirical model formulations.

CONCLUSIONS

We suggest that choice of hydrothermal model should depend on the objectives of the study or application. If accurate prediction of germination time in a complex field environment is the objective, then the PO model is less accurate than the REG or SG models. Accurate rate estimation is a key feature of rate-sum indices that interpret seedlot performance through interpretation of actual field response. If computational efficiency is an important factor, then optimized regression techniques are desirable, as those procedures require relatively little effort to optimize and test equations across multiple seedlots and subpopulations. Optimized regression models, however, require relatively more data to parameterize and are often not able to predict germination rate of later-germinating subpopulations. Despite generally lower model accuracy, the PO model has the unique advantage of generating model coefficients that can be used for qualitative ranking of seedlots and to give information for more detailed investigations into the physiological mechanisms behind population variability in germination rate.

References

Allen, P. 2003. When and how many? Hydrothermal models and the prediction of seed germination. New Phytol. 158:1–3. doi:10.1046/j.1469-8137.2003.00729.x

Allen, P.S., and S.E. Meyer. 1998. Ecological aspects of seed dormancy loss. Seed Sci. Res. 8:183–191. doi:10.1017/S0960258500004098

Allen, P.S., S.E. Meyer, and M.A. Khan. 2000. Hydrothermal time as a tool in comparative germination studies. In: M. Black, K.J. Bradford, and J. Vazquez-Ramos, editors, Seed biology: Advances and applications. CAB International, Wallingford, UK. p. 401–410.

Alvarado, V., and K.J. Bradford. 2002. A hydrothermal time model explains the cardinal temperatures for seed germination. Plant Cell Environ. 25:1061–1069. doi:10.1046/j.1365-3040.2002.00894.x

Arnold, C.Y. 1959. The determination and significance of the base temperature in a linear heat unit system. J. Am. Soc. Hortic. Sci. 74:430–445.

Batlla, D., and R.L. Benech-Arnold. 2003. A quantitative analysis of dormancy loss dynamics in *Polygonium aviculare* L. seeds: Development of a thermal time model based on changes in seed population thermal parameters. Seed Sci. Res. 13:55–68. doi:10.1079/SSR2002124

Bauer, M.C., S.E. Meyer, and P.S. Allen. 1998. A simulation model to predict seed dormancy loss in the field for *Bromus tectorum* L. J. Exp. Bot. 49:1235–1244.

Bloomberg, M., J.R. Sedcole, E.G. Mason, and G. Buchan. 2009. Hydrothermal time models for radiata pine (*Pinus radiata* D. Don). Seed Sci. Res. 19:171–182. doi:10.1017/S0960258509990031

Boddy, L.G., K.J. Bradford, and A.J. Fischer. 2012. Population based threshold models describe weed germination and emergence patterns across varying temperature, moisture and oxygen conditions. J. Appl. Ecol. 49:1225–1236. doi:10.1111/j.1365-2664.2012.02206.x

Bradford, K.J. 1990. A water relations analysis of seed germination rates. Plant Physiol. 94:840–849. doi:10.1104/pp.94.2.840

Brown, R.F., and D.G. Mayer. 1988. Representing cumulative germination. 1. Germination indices. Ann. Bot. (Lond.) 61:117–125.

Call, C.A., and B.A. Roundy. 1991. Perspectives and processes in revegetation of arid and semiarid rangelands. J. Range Manage. 44:543–549. doi:10.2307/4003034

Cheng, Z., and K.J. Bradford. 1999. Hydrothermal time analysis of tomato seed germination responses to priming treatments. J. Exp. Bot. 50:89–99. doi:10.1093/jxb/50.330.89

Christensen, M., S.E. Meyer, and P.S. Allen. 1996. A hydrothermal time model of seed after-ripening in *Bromus tectorum* L. Seed Sci. Res. 6:155–163. doi:10.1017/S0960258500003214

Covell, S., R.H. Ellis, E.H. Roberts, and R.J. Summerfield. 1986. The influence of temperature on seed germination rate in grain legumes. I. A comparison of chickpea, lentil, soyabean and cowpea at constant temperatures. J. Exp. Bot. 37:705–715. doi:10.1093/jxb/37.5.705

Dahal, P., and K.J. Bradford. 1994. Hydrothermal time analysis of tomato seed germination at suboptimal temperature and reduced water potential. Seed Sci. Res. 4:71–80. doi:10.1017/S096025850000204X

Ellis, R.H., S. Covell, E.H. Roberts, and R.J. Summerfield. 1986. The influence of temperature on seed germination rate in grain legumes. II. Interspecific variation in chickpea (*Cicer arietinum* L.) at constant temperature. J. Exp. Bot. 37:1503–1515. doi:10.1093/jxb/37.10.1503

Ellis, R.H., G. Simon, and S. Covell. 1987. The influence of temperature on seed germination rate in legumes. III. A comparison of five faba bean genotypes at constant temperatures using a new screening method. J. Exp. Bot. 38:1033–1043. doi:10.1093/jxb/38.6.1033

Finch-Savage, W.E., and K. Phelps. 1993. Onion (*Allium cepa* L.) seedling emergence patterns can be explained by the influence of soil temperature and water potential on seed germination. J. Exp. Bot. 44:407–414. doi:10.1093/jxb/44.2.407

Finch-Savage, W.E., J.R.A. Steckel, and K. Phelps. 1998. Germination and post-germination growth to carrot seedling emergence: Predictive threshold model and sources of variation between sowing occasions. New Phytol. 139:505–516. doi:10.1046/j.1469-8137.1998.00208.x

Flerchinger, G.N., T.G. Caldwell, J. Cho, and S.P. Hardegree. 2012. Simultaneous heat and water (SHAW) model: Model use, calibration and validation. Trans. ASABE 55:1395–1411. doi:10.13031/2013.42250

Garcia-Huidobro, J., J.L. Monteith, and G.R. Squire. 1982a. Time, temperature and germination of pearl millet (*Pennisetum typhoides* S. & H.). I. Constant temperature. J. Exp. Bot. 33:288–296. doi:10.1093/jxb/33.2.288

Garcia-Huidobro, J., J.L. Monteith, and G.R. Squire. 1982b. Time, temperature and germination of pearl millet (*Pennisetum typhoides* S. & H.). II. Alternating temperature. J. Exp. Bot. 33:297–302. doi:10.1093/jxb/33.2.297

Grubb, P.J. 1977. The maintenance of species-richness in plant communities: The importance of regeneration niche. Biol. Rev. Camb. Philos. Soc. 52:107–145. doi:10.1111/j.1469-185X.1977.tb01347.x

Grundy, A.C., K. Phelps, R.J. Reader, and S. Burston. 2000. Modelling the germination of *Stellaria media* using the concept of hydrothermal time. New Phytol. 148:433–444. doi:10.1046/j.1469-8137.2000.00778.x

Gummerson, R.J. 1986. The effect of constant temperatures and osmotic potentials on the germination of sugar beet. J. Exp. Bot. 37:729–741. doi:10.1093/jxb/37.6.729

Hardegree, S.P. 2006a. Predicting germination response to temperature. I. Cardinal-temperature models and subpopulation-specific regression. Ann. Bot. (Lond.) 97:1115–1125. doi:10.1093/aob/mcl071

Hardegree, S.P. 2006b. Predicting germination response to temperature. III. Model validation under field-variable temperature conditions. Ann. Bot. (Lond.) 98:827–834. doi:10.1093/aob/mcl163

Hardegree, S.P., G.N. Flerchinger, and S.S. Van Vactor. 2003. Hydrothermal germination response and the development of probabilistic germination profiles. Ecol. Modell. 167:305–322. doi:10.1016/S0304-3800(03)00192-3

Hardegree, S.P., T.A. Jones, B.A. Roundy, N.L. Shaw, and T.A. Monaco. 2011. Assessment of range planting as a conservation practice. In: D.D. Briske, editor, Conservation benefits of rangeland practices: Assessment, recommendations, and knowledge gaps. Allen Press, Lawrence, KS. p. 171–212.

Hardegree, S.P., C.A. Moffet, G.N. Flerchinger, J. Cho, B.A. Roundy, T.A. Jones, J.J. James, P.E. Clark, and F.B. Pierson. 2013. Hydrothermal assessment of temporal variability in seedbed microclimate. Rangeland Ecol. Manag. 66:127–135. doi:10.2111/REM-D-11-00074.1

Hardegree, S.P., and S.S. Van Vactor. 1999. Predicting germination response of four cool-season range grasses to field-variable temperature regimes. Environ. Exp. Bot. 41:209–217. doi:10.1016/S0098-8472(99)00004-0

Hardegree, S.P., and S.S. Van Vactor. 2000. Germination and emergence of primed grass seeds under field and simulated-field temperature regimes. Ann. Bot. (Lond.) 85:379–390. doi:10.1006/anbo.1999.1076

Hardegree, S.P., S.S. Van Vactor, F.B. Pierson, and D.E. Palmquist. 1999. Predicting variable-temperature response of non-dormant seeds from constant-temperature germination data. J. Range Manage. 52:83–91. doi:10.2307/4003496

Hardegree, S.P., and A.H. Winstral. 2006. Predicting germination response to temperature. II. Three-dimensional regression,

statistical gridding and iterative probit optimization using measured and interpolated-subpopulation data. Ann. Bot. (Lond.) 98:402–410.

Kebreab, E., and A.J. Murdoch. 1999. Modelling the effects of water stress and temperature on germination rate of *Orobanche aegyptiaca* seeds. J. Exp. Bot. 50:655–664. doi:10.1093/jxb/50.334.655

Köchy, M., and K. Tielbörger. 2007. Hydrothermal time model of germination: Parameters for 36 Mediterranean annual species based on a simplified approach. Basic Appl. Ecol. 8:171–182. doi:10.1016/j.baae.2006.04.002

Meyer, S.E., and P.S. Allen. 2009. Predicting seed dormancy loss and germination timing for *Bromus tectorum* in a semi-arid environment using hydrothermal time models. Seed Sci. Res. 19:225–239. doi:10.1017/S0960258509990122

Peters, D.P.C. 2000. Climatic variation and simulated patterns in seedling establishment of two dominant grasses at a semi-arid-arid grassland ecotone. J. Veg. Sci. 11:493–504. doi:10.2307/3246579

Phelps, K., and W.E. Finch-Savage. 1997. A statistical perspective on threshold-type germination models. In: R.H. Ellis, M. Black, A.J. Murdoch, and T.D. Hong, editors, Basic and applied aspects of seed biology. Kluwer Acad. Publ., Dordrecht. p. 361–368.

Roman, E.S., A.G. Thomas, S.D. Murphy, and C.J. Swanton. 1999. Modeling germination and seedling elongation of common lambsquarters (*Cenopodium album*). Weed Sci. 47:149–155.

Roundy, B.A., and S.H. Biedenbender. 1996. Germination of warm-season grasses under constant and dynamic temperatures. J. Range Manage. 49:425–431. doi:10.2307/4002924

Rowse, H.R., and W.E. Finch-Savage. 2003. Hydrothermal threshold models can describe the germination response of carrot (*Daucus Carota*) and onion (*Allium cepa*) seed populations across both sub- and supra-optimal temperatures. New Phytol. 158:101–108. doi:10.1046/j.1469-8137.2003.00707.x

Scott, S.J., R.A. Jones, and W.A. Williams. 1984. Review of data analysis methods for seed germination. Crop Sci. 24:1192–1199. doi:10.2135/cropsci1984.0011183X002400060043x

Wang, R., Y. Bai, and K. Tanino. 2005. Germination of winterfat [*Eurotia lanata* (Pursh) Moq.] seeds at reduced water potentials: Testing assumptions of hydrothermal time model. Environ. Exp. Bot. 53:49–63. doi:10.1016/j.envexpbot.2004.03.001